

Topological electric current from time-dependent elastic deformations in grapheneAbolhassan Vaezi,^{1,2} Nima Abedpour,² Reza Asgari,^{2,*} Alberto Cortijo,³ and María A. H. Vozmediano³¹*Department of Physics, Cornell University, Ithaca, New York 14853, USA*²*School of Physics, Institute for Research in Fundamental Sciences, IPM, Tehran 19395-5531, Iran*³*Instituto de Ciencia de Materiales de Madrid, CSIC, Cantoblanco, 28049 Madrid, Spain*

(Received 30 April 2013; published 3 September 2013)

We show the possibility of inducing an edge charge current by applying time-dependent strain in gapped graphene samples preserving time-reversal symmetry. We demonstrate that this edge current has the same origin as the valley Hall response known to exist in the system.

DOI: [10.1103/PhysRevB.88.125406](https://doi.org/10.1103/PhysRevB.88.125406)

PACS number(s): 72.80.Vp, 61.48.Gh, 73.43.Cd, 81.40.Jj

I. INTRODUCTION

Topological insulators^{1,2} are a hallmark of the condensed-matter physics of the 21st century. They realize a new state of matter characterized by topology rather than symmetry. The topologically nontrivial character is strongly related to the discrete symmetries of the band Hamiltonian such as time-reversal symmetry (TRS), inversion, or parity. It has observable consequences in the form of nondissipative currents at the edge of the sample or, equivalently, quantized transverse electric responses to external electromagnetic probes such as the quantum Hall conductivity σ_{xy} .³

The quantum Hall example led to the assumption that breaking TRS was an essential ingredient for the observation of topological phenomena which will not occur in insulators preserving TRS. The reason is clear: the Hall conductivity is proportional to the integral over the Brillouin zone of the Berry connection which is zero in time-reversal-invariant systems.¹ The proposals of Semenoff and Haldane^{4,5} of getting Landau levels in a system with zero applied magnetic field followed by the description of the quantum spin Hall effect^{6,7} paved the way to the development of the actual field of topological insulators. The spin Hall effect was the first example of a topological response in a TRS-invariant system and is based on the recognition that the presence of additional degrees of freedom (spin in this case) allows us to define different types of masses that give rise to other topological currents.^{8,9}

Graphene,^{10–12} the best example of Dirac fermions with extra quantum numbers (spin, valley, layer), is the ideal model to test this type of quantized responses. The neutral system has two inequivalent Fermi points (valleys) located at the corners of the Brillouin zone. Because of their large separation in momentum space, intervalley scattering is strongly suppressed, and in the absence of short-range disorder or interactions the valley index remains a good quantum number. In these circumstances a valley Hall effect can occur similar to the spin Hall effect where carriers in different valleys flow to opposite transverse edges driven by an in-plane external electric field. The valley Hall effect was already discussed in the early times of graphene,¹³ and “valleytronics” applications were proposed.¹⁴ Valley currents induced by ac fields or optical radiation have been experimentally realized in various materials.^{15–17}

One of the most interesting aspects of graphene is the tight relation between electronic excitations and mechanical deformations of the lattice. In the very successful tight-

binding–elasticity approach, lattice deformations couple to the electronic current in the form of gauge fields and scalar potentials very similar to the usual electromagnetic gauge potential.^{18,19} Time-dependent strains give rise to a “synthetic” electric field that will play a major role in the present work. In the valley Hall effect there is no charge accumulation at the edges because the external electric field couples with the same sign to both valleys. We will show that a charge current can be generated from time-dependent elastic deformations not breaking TRS in graphene. The result lies on a mixed Chern-Simons term in the effective action that involves the electromagnetic and the elastic vector potentials. The interplay of strain and valley physics has been explored previously,^{20–22} and some consequences of having time-dependent strain in graphene were considered.^{23–26}

This paper is organized as follows. In Sec. II we introduce the formalism that will be used in calculating the topological current. In Sec. III we present our analytical and numerical results for suggesting an experimental realization in time-dependent strained graphene sheets. Section IV contains discussions and conclusions.

II. THE MODEL AND THEORY

In the absence of lattice deformations the low-energy electronic degrees of freedom around the two Fermi points in graphene can be described by a massless Dirac Hamiltonian.¹²

$$H(\mathbf{k}) = \sum_{\tau} \psi_{\tau,\mathbf{k}}^{\dagger} (\tau \sigma_x k_x + \sigma_y k_y) \psi_{\tau,\mathbf{k}}, \quad (1)$$

where $\tau = \pm 1$ refers to the two Fermi points and $\psi_{\tau,\mathbf{k}}$ represents two species of spinors. The Fermi velocity will not play a role in our discussion and has been set to 1 as well as \hbar . The time-reversal-symmetry operation interchanges the two species of spinors, keeping Eq. (1) time reversal invariant. An essential ingredient for the quantized response is the presence of a gap in the spectrum. In the quantum Hall effect the insulating behavior is induced by the perpendicular magnetic field. When spins are neglected, there are essentially four ways of opening a gap in the otherwise linear spectrum of Eq. (1).²⁷ Three of them are time reversal invariant and physically correspond to inducing a different on-site potential for the two sublattices or coupling the degrees of freedom to a Kekulé distortion. The corresponding mass has the same sign for both Fermi points. The fourth one breaks time-reversal

symmetry and was used by Haldane in his proposal for the anomalous quantum Hall effect in the honeycomb lattice.⁵ We will restrict ourselves to the first mass mentioned above,

$$H_m = m\psi_{\tau,\mathbf{k}}^+ \sigma_3 \psi_{\tau,\mathbf{k}}, \quad (2)$$

and discuss later on the possible mechanism to generate this term in real samples.

As discussed extensively in Ref. 19, a deformation of the graphene lattice gives rise to a fictitious gauge field,

$$\mathbf{A}^{el} = \frac{\kappa\Phi_0}{\pi} \begin{pmatrix} u_{xx} - u_{yy} \\ -2u_{xy} \end{pmatrix}, \quad (3)$$

where $\kappa \simeq 3 \text{ nm}^{-1}$, Φ_0 is the flux quantum, and u_{ij} is the strain tensor, which can be written as $u_{ij} = \frac{1}{2}[\partial_j u_i + \partial_i u_j + (\partial_i h)(\partial_j h)]$ in terms of the in-plane and out-of-plane displacements \mathbf{u} and h , respectively. This field couples minimally to the electronic excitations with opposite signs to the two valleys. Hence in the presence of an external electromagnetic and elastic field the interacting Hamiltonian reads

$$H_A = - \sum_{\tau} [\psi_{\tau,\mathbf{k}}^+ \tau \sigma_x (eA_x^{em} + \tau \hat{\beta} A_x^{el}) \psi_{\tau,\mathbf{k}}] - \sum_{\tau} [\psi_{\tau,\mathbf{k}}^+ \sigma_y (eA_y^{em} + \tau \hat{\beta} A_y^{el}) \psi_{\tau,\mathbf{k}}], \quad (4)$$

where e is the electric charge, \mathbf{A}^{em} and \mathbf{A}^{el} stand for the electromagnetic and the elastic vector fields, respectively, and we have encoded the strength of the elastic coupling in the parameter $\hat{\beta} > 0$. Note that we multiply \mathbf{A}^{el} by τ in Eq. (4) since the two valleys couple with opposite charges to the strain. This is due to the fact that the strain gauge field \mathbf{A}^{el} respects the time-reversal symmetry under which the K and the K' valleys will be interchanged.

A. The topological current

In order to obtain the topological response of a gapped system to external gauge fields, we must find its topological indices. For example, if quasiparticles of the system couple to a gauge field with charge q , the off-diagonal conductance of the system depends on the first Chern number C as $\sigma_{xy} = Cq^2/h$. The Chern number can itself be computed through integrating the Berry curvature of the ground state over the momentum space. For example, the Berry curvature for a two-band system with $\mathcal{M}_k = \vec{d}_k \cdot \vec{\sigma}$ Hamiltonian reads²⁹

$$\mathcal{F}_{xy} = \frac{1}{2} \hat{d}_k \cdot (\partial_{k_x} \hat{d} \times \partial_{k_y} \hat{d}). \quad (5)$$

where $\hat{k} = \vec{k}/|k|$. Since a gapped graphene can be viewed as two massive Dirac cones, we first compute the response of a single one. Consider a generic Dirac cone with the $\mathcal{M}_k = v_F(\eta_x k_x \sigma_x + \eta_y k_y \sigma_y) + m\sigma_z$ Hamiltonian, where η_x and η_y take ± 1 values. Therefore, $\vec{k} = (\eta_x v_F k_x, \eta_y v_F k_y, m)$. Using the corresponding \hat{k} and plugging it in Eq. (5), the Chern number reads

$$C = \frac{1}{2} \text{sgn}(m\eta_x\eta_y). \quad (6)$$

Therefore, in the gapped system with the mass term given in Eq. (2) the band structure around each Fermi point is topologically characterized by a Chern number which takes

opposite values at the two Fermi points (due to the time-reversal symmetry):^{28,29}

$$C_{\mathbf{K}} = -C_{\mathbf{K}'} = \text{sgn}(m)/2. \quad (7)$$

In the absence of elastic deformations as a response to an external electric field \mathbf{E}^{em} the induced charge current at each Fermi point is

$$\langle J_{\tau}^i \rangle = e^2 C_{\tau} \varepsilon^{ij} E_j^{em}, \quad (8)$$

so the total charge current $\langle J_{\mathbf{K}}^i + J_{\mathbf{K}'}^i \rangle$ vanishes. However, there is still a topological response encoded in the quantity $\langle J_{\mathbf{K}}^i - J_{\mathbf{K}'}^i \rangle$ which is not zero and physically represents a current imbalance between the two Fermi points; this is the manifestation of the quantum valley Hall effect.

Consider now a time-dependent elastic deformation described by a vector field $\mathbf{A}^{el}(t)$ such as the one described in the previous section. Its associated synthetic electric field $E_j^{el} = \partial_i A_j^{el}(t)$ will couple with opposite signs to the two valleys. Hence this type of deformation will induce a charge response in the system at each Fermi point:

$$\langle J_{\tau}^i \rangle \sim \tau C_{\tau} \varepsilon^{ij} E_j^{el}. \quad (9)$$

Now, because $C_{\mathbf{K}} = -C_{\mathbf{K}'}$ the total net charge current is nonzero and its value is two times larger than the value at each Fermi point,

$$\langle J_{\mathbf{K}}^i + J_{\mathbf{K}'}^i \rangle \sim 2C_{\mathbf{K}} \varepsilon^{ij} E_j^{el}. \quad (10)$$

We can make this statement more formal by considering the effective background field theory.⁹ Within a functional integral approach one can integrate out the fermionic degrees of freedom $\psi_{\tau,\mathbf{k}}, \psi_{\tau,\mathbf{k}}^+$ in the action derived from Eq. (4) and write the odd part of the effective Lagrangian:

$$\mathcal{L}_{\text{eff}} = 2e\hat{\beta}C_{\mathbf{K}}\varepsilon^{\mu\rho\nu}A_{\mu}^{em}\partial_{\rho}A_{\nu}^{el} + 2e\hat{\beta}C_{\mathbf{K}}\varepsilon^{\mu\rho\nu}A_{\mu}^{el}\partial_{\rho}A_{\nu}^{em} + J^{\mu}A_{\mu}^{em} + J_{el}^{\mu}A_{\mu}^{el}, \quad (11)$$

where we have added to the Chern-Simons action the external sources: J^{μ} is the total charge density current that naturally couples to the electromagnetic field, and J_{el}^{μ} is a classically conserved current associated with the elastic field A_{μ}^{el} . Notice that the standard Chern-Simons term bilinear in A^{em} or A^{el} vanishes for the total action due to the opposite value of $C_{\mathbf{K}}$ at the two valleys. Only the mixed term survives.

From Eq. (11) we can immediately read out the total charge current density ($\mathcal{S}_{\text{eff}} = \int d^3\mathcal{L}_{\text{eff}}$):

$$\langle J^i \rangle = \frac{\delta\mathcal{S}_{\text{eff}}}{\delta A_i^{em}} = 2e\hat{\beta}C_{\mathbf{K}}\varepsilon^{ij}\dot{A}_j^{el} \equiv 2e\hat{\beta}\frac{m}{|m|}\varepsilon^{ij}E_j^{el}, \quad (12)$$

where we have assumed for simplicity that $A_0^{el} = 0$ and have replaced $\varepsilon^{ij0} = \varepsilon^{ij}$.

Equation (12) is the main result of this work. A nonvanishing net charge current density can be obtained as a response to a time-dependent elastic deformation of the gapped graphene sample. Notice that this equation is consistent with time-reversal symmetry because, as we emphasized previously, the synthetic electric field is odd under time reversal.³⁰

This result is the counterpart of the quantum valley Hall effect. In Fig. 1 we represent schematically a comparison between the Hall effect, the valley Hall effect, and the effect

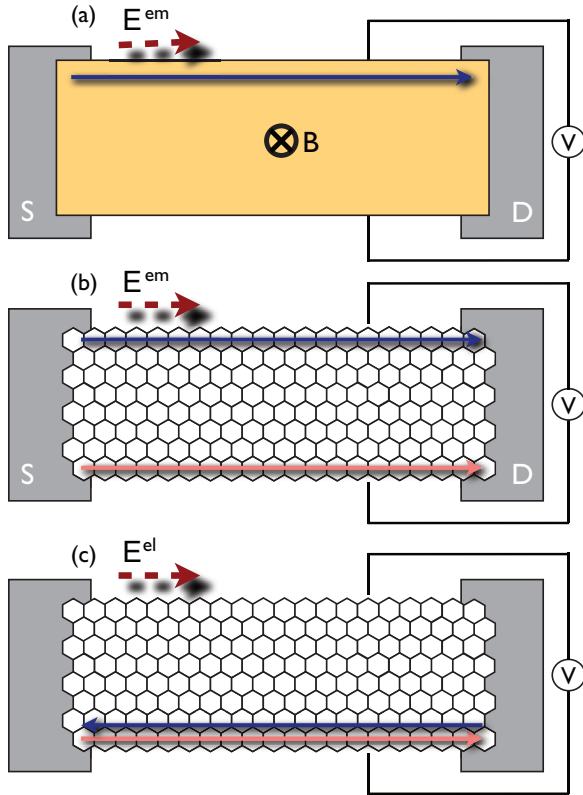


FIG. 1. (Color online) Comparison between (a) the Hall effect, (b) the valley Hall effect, and (c) the effect proposed in the text following the scheme of the original implementation of the experiment first proposed by Hall. The arrows indicate the flow of valley polarized electrons under the action of an external electric field or voltage [(a) and (b)] and of a time-dependent strain [in (c)]. In the latter case the total current is $\langle J_K^i + J_{K'}^i \rangle \sim E_j^{el}$.

proposed in the text. Figure 1(a) shows the original implementation of the experiment first proposed by Hall.³¹ In the presence of a magnetic field perpendicular to the sample and a voltage difference along the x direction the charge carriers are deflected to one of the edges of the sample. The charge accumulation in one side gives a voltage difference between the two samples' edges in the y direction. In the valley Hall effect [Fig. 1(b)] there is no magnetic field. The electromotive force acts along the x direction, but now the electrons crossing the sample find two channels to flow, one at each sample's edge. The voltage difference between the two edges is now zero, but the carriers flowing along different edges belong to different valleys or Fermi points, so there is a net valley imbalance between the edges in the y direction. Finally, the charge effect proposed in this work is shown in Fig. 1(c). The external probe now is a time-dependent elastic deformation creating a synthetic electric field along the x direction. Electrons belonging to different valleys react oppositely to this electromotive elastic force, so the two available channels belong to the same edge, and a net charge accumulation occurs in one of the two sides of the sample. Hence a net voltage difference appears between the edges. Because both channels belong to different Fermi points, no valley imbalance appears in this situation.

III. SUGGESTED EXPERIMENTAL REALIZATION

A potential experimental setup to measure the effect described in this work needs a gapped graphene system with reasonably well defined zigzag edges. We also need to induce time-dependent strain, but there is no need for high control on this part. One possibility is to use the proposal of Refs. 32 and 33, where graphene is grown on a thin copper substrate with outstanding flexibility. The strain on the graphene sample can be controlled by manipulating the substrate. The sample can be gapped by chemical doping as done in Ref. 34, although the needed gap could also be induced by the strain field as described in Ref. 21.

The vector field induced by an elastic deformation of the graphene lattice is given in Eq. (3). A possible strain configuration is shown in Fig. 2. The left-hand side shows the atomic displacements given by $(u_x, u_y) = (-2P_Bxy + P_E(t)y^2, P_B(x^2 + y^2))$ in Cartesian coordinates. P_B and $P_E(t)$ are geometric parameters with units of $1/\text{length}$, and $P_E(t)$ is a time-varying periodic function, for instance, $P_E(t) = P_B \cos(\omega t)$. This particular strain leads to a uniform magnetic field $\tilde{B}_z = 4\phi_0 c\beta P_B/a$ and pseudoelectric field $\tilde{E}_y = -2\phi_0 c\beta\omega \sin(\omega t)y/a$. To simplify the analysis the strain has been chosen such that the induced scalar potential which is proportional to $u_{xx} + u_{yy}$ vanishes. Neither this condition nor the uniform pseudomagnetic field is necessary for the proposed mechanism to work, but they provide a neat setting for the discussion. A value of $P_B = 0.5 \mu\text{m}^{-1}$ in a sample of size $0.4 \mu\text{m} \times 0.4 \mu\text{m}$ gives a pseudomagnetic field of $\tilde{B}_z \approx 9.0T$, which is large enough to give rise to quantized Landau levels. The sample can be tailored in the form of a ribbon with zigzag termination such that there will be edge states with a good valley number.³⁵ The experimental possibility of tailoring proper edges has been demonstrated in Ref. 36. As we discussed above, an external electric field cannot induce a current along the horizontal boundaries, but the pseudoelectric field given by $-\partial\mathbf{A}_{el}(t)/\partial t$ easily creates a voltage along the boundaries, as shown on the right-hand side of Fig. 2. Using a reasonable value for the parameters and $\omega = 60 \text{ MHz}$, the maximum pseudoelectric field reaches 50 V/m , and then J_x would be about $4 \times 10^{-3} \text{ A/m}$. This induced current can be measured by experiments.

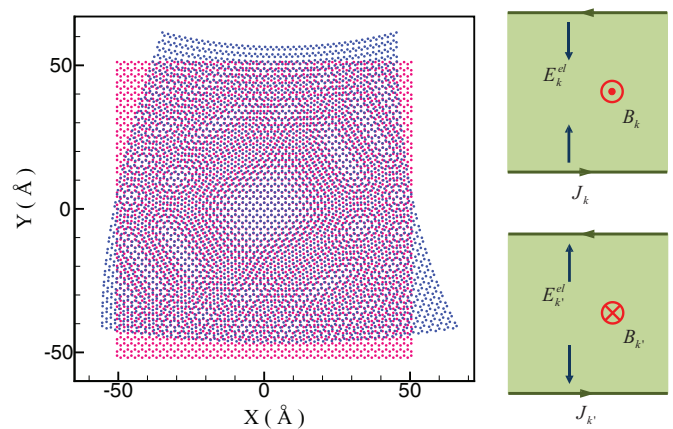


FIG. 2. (Color online) (left) Proposed strain for a graphene ribbon as described in the main text. (right) Direction of the charge current for the two Dirac points in different edges.

Bilayer graphene³⁷ is another possible system, perhaps better than the monolayer, to observe the proposed current. The gated graphene bilayer is known to be another realization of a quantum valley Hall insulator, whose low-energy theory is exactly the same mixed Chern-Simons theory described in our work. The system is gapped when a gate voltage is applied between the two graphene layers, and it supports the same structure of valley resolved edge states. As in its monolayer counterpart, having zigzag edge states is essential to develop such edge states. However, contrary to the case of monolayer graphene, a subgap conduction in gated graphene bilayer ribbons has been experimentally reported.³⁸ This subgap conductance has been attributed to the presence of edge states in the sample, indicating that the conduction along the edge states survives even when there is no perfect zigzag crystalline ordering at the edges.³⁹ Quantum manipulation of valleys in bilayer graphene has been reported recently.⁴⁰

IV. CONCLUSIONS

We have shown that a nonvanishing charge current can be generated in gapped graphene by applying time-dependent strain. Unlike the standard Hall effect proportional to e^2 , its coefficient is proportional to the product of the electric charge times an elastic constant characteristic of graphene $\hat{\beta}$. The proposed mechanism is a consequence of the mixed responses that can be obtained in nontrivial topological Dirac systems when several vector fields are coupled. The proposed effect can be measured in actual graphene devices or in alternative systems such as artificial graphene⁴¹ or optical lattices.⁴²

ACKNOWLEDGMENTS

We wish to thank A. Concha, M. Barkeshli, and A. G. Grushin for useful discussions. This research was supported in part by the Spanish MEC D Grants No. FIS2011-23713 and No. PIB2010BZ-00512.

*asgari@ipm.ir

¹M. Z. Hasan and C. L. Kane, *Rev. Mod. Phys.* **82**, 3045 (2010).

²X. Qi and S. Zhang, *Rev. Mod. Phys.* **83**, 1057 (2011).

³K. Von Klitzing, G. Dorda, and M. Pepper, *Phys. Rev. Lett.* **45**, 494 (1980).

⁴G. W. Semenoff, *Phys. Rev. Lett.* **53**, 2449 (1984).

⁵F. D. M. Haldane, *Phys. Rev. Lett.* **61**, 2015 (1988).

⁶C. L. Kane and E. J. Mele, *Phys. Rev. Lett.* **95**, 226801 (2005).

⁷B. A. Bernevig and S. C. Zhang, *Phys. Rev. Lett.* **96**, 106802 (2006); G. E. Volovik, *JETP* **67**, 1804 (1988).

⁸S. Ryu, C. Mudry, C. Y. Hou, and C. Chamon, *Phys. Rev. B* **80**, 205319 (2009).

⁹A. Cortijo, A. G. Grushin, and M. A. H. Vozmediano, *Phys. Rev. B* **82**, 195438 (2010).

¹⁰K. S. Novoselov, A. K. Geim, S. V. Morozov, D. Jiang, M. I. Katsnelson, I. V. Grigorieva, S. V. Dubonos, and A. A. Firsov, *Nature (London)* **438**, 197 (2005).

¹¹Y. Zhang, Y.-W. Tan, H. L. Stormer, and P. Kim, *Nature (London)* **438**, 201 (2005).

¹²A. H. Castro Neto, F. Guinea, N. M. R. Peres, K. S. Novoselov, and A. K. Geim, *Rev. Mod. Phys.* **81**, 109 (2009).

¹³D. Xiao, W. Yao, and Q. Niu, *Phys. Rev. Lett.* **99**, 236809 (2007).

¹⁴A. Rycerz, J. Tworzydło, and C. W. J. Beenakker, *Nat. Phys.* **3**, 172 (2007).

¹⁵J. Karch, S. A. Tarasenko, E. L. Ivchenko, J. Kamann, P. Olbrich, M. Utz, Z. D. Kvon, and S. D. Ganichev, *Phys. Rev. B* **83**, 121312(R) (2011).

¹⁶H. Zeng, J. Dai, W. Yao, D. Xiao, and X. Cui, *Nat. Nanotechnol.* **7**, 490 (2012).

¹⁷K. F. Mak, K. He, J. Shan, and T. F. Heinz, *Nat. Nanotechnol.* **7**, 494 (2012).

¹⁸H. Suzuura and T. Ando, *Phys. Rev. B* **65**, 235412 (2002).

¹⁹M. A. H. Vozmediano, M. I. Katsnelson, and F. Guinea, *Phys. Rep.* **493**, 109 (2010).

²⁰F. Guinea, M. I. Katsnelson, and M. A. H. Vozmediano, *Phys. Rev. B* **77**, 075422 (2008).

²¹F. Guinea, M. I. Katsnelson, and A. G. Geim, *Nat. Phys.* **6**, 30 (2010).

²²Z. G. Zhu and J. Berakdar, *Phys. Rev. B* **84**, 195460 (2011).

²³F. von Oppen, F. Guinea, and E. Mariani, *Phys. Rev. B* **80**, 075420 (2009).

²⁴N. E. Firsova and Y. A. Firsov, *J. Phys. D* **45**, 435102 (2012).

²⁵Y. Jiang, T. Low, K. Chang, M. I. Katsnelson, and F. Guinea, *Phys. Rev. Lett.* **110**, 046601 (2013).

²⁶T. Iadecola, D. Campbell, C. Chamon, C. Y. Hou, R. Jackiw, S. Y. Pi, and S. V. Kusminskiy, *Phys. Rev. Lett.* **110**, 176603 (2013).

²⁷A. Cortijo, F. Guinea, and M. A. H. Vozmediano, *J. Phys. A* **45**, 383001 (2012).

²⁸X. G. Wen, *Int. J. Mod. Phys. B* **5**, 1641 (1991).

²⁹X.-G. Wen, *Quantum Field Theory of Many-Body Systems: From the Origin of Sound to an Origin of Light and Electrons* (Oxford University Press, Oxford, 2004).

³⁰We thank A. G. Grushin for extensive discussions around this point.

³¹E. Hall, *Am. J. Math.* **2**, 287 (1879).

³²S. Bae *et al.*, *Nat. Nanotechnol.* **5**, 574 (2010).

³³K. S. Kim, Y. Zhao, H. Jang, S. Y. Lee, J. M. Kim, K. S. Kim, J. H. Ahn, P. Kim, J. Y. Choi, and B. H. Hong, *Nature (London)* **457**, 706 (2009).

³⁴D. C. Elias, R. R. Nair, T. M. G. Mohiuddin, S. V. Morozov, P. Blake, M. P. Halsall, A. C. Ferrari, D. W. Boukhvalov, M. I. Katsnelson, A. K. Geim *et al.*, *Science* **323**, 610 (2009).

³⁵T. Low and F. Guinea, *Nano Lett.* **10**, 3551 (2010).

³⁶L. C. Campos, V. R. Manfrinato, J. D. Sanchez-Yamagishi, J. Kong, and P. Jarillo-Herrero, *Nano Lett.* **9**, 2600 (2009).

³⁷E. V. Castro, K. S. Novoselov, S. V. Morozov, N. M. R. Peres, J. Lopes dos Santos, J. Nilsson, F. Guinea, A. K. Geim, and A. H. Castro Neto, *Phys. Rev. Lett.* **99**, 216802 (2006).

³⁸J. Li, I. Martin, M. Buttiker, and A. F. Morpurgo, *Nat. Phys.* **7**, 38 (2011).

³⁹A. Vaezi, Y. Liang, D. H. Ngai, L. Yang, and E. A. Kim, *Phys. Rev. X* **3**, 021018 (2013).

⁴⁰G. Y. Wu, N. Lue, and Y. Chen, arXiv:1302.1318 (unpublished).

⁴¹K. K. Gomes, W. Mar, W. Ko, F. Guinea, and H. C. Manoharan, *Nature (London)* **483**, 306 (2012).

⁴²K. L. Lee, B. Gremaud, R. Han, B. G. Englert, and C. Miniatura, *Phys. Rev. A* **80**, 043411 (2009).